Preprints of the 21st IFAC World Congress (Virtual)
Berlin, Germany, July 12-17, 2020

Hyperspherical Unscented Particle Filter for Nonlinear Orientation Estimation

Kailai Li, Florian Pfaff, and Uwe D. Hanebeck

Intelligent Sensor-Actuator-Systems Laboratory (ISAS)
Institute for Anthropomatics and Robotics
Karlsruhe Institute of Technology (KIT), Germany
kailai.li@kit.edu, florian.pfaff@kit.edu, uwe.hanebeck@kit.edu

Abstract: We propose a novel quaternion particle filter for nonlinear SO(3) estimation. For importance sampling, the proposal distribution is designed to incorporate newly observed evidence. For that, the unscented Kalman filtering is performed particle-wise on the tangent plane of the unit quaternion manifold via gnomonic projection/retraction based on hyperspherical geometry. As prior particles are driven towards high-likelihood regions on the manifold, computational efficiency of quaternion particle filtering is significantly improved. The resulting hyperspherical unscented particle filter (HUPF) is evaluated for nonlinear orientation estimation in simulations. Results show that it gives superior tracking performance compared with the conventional particle filter and other existing quaternion filtering schemes relying on parametric modeling.

Keywords: Parameter estimation, information fusion, recursive Bayesian filtering, directional estimation, unscented particle filter, hyperspherical geometry.

1. INTRODUCTION

Orientation estimation plays a key role in many application scenarios, such as autonomous driving, computer vision, robotic control, etc (see works from Li et al. (2020); Hashim et al. (2019); Pfaff et al. (2020); Möls et al. (2020) for an overview). However, accurate and robust recursive orientation estimation is not trivial. For instance, various options exist for parameterizing three-DoF spatial orientations. Euler angles provide a minimal representation, yet suffer from gimbal lock. This ambiguity can be overcome by employing the well-known rotation matrices. However, the over-parameterization also introduces a large degree of redundancy (nine elements are used for representing the three DoF), leading to memory inefficiency and numerical instability. One popular alternative are unit quaternions, which provide a re-parameterization of the axis-angle representation. Commonly, unit quaternions are expressed as four-dimensional vectors, and thus only have one degree of redundancy and no ambiguity. In this paper, we exploit unit quaternions as the state representation for recursive orientation estimation.

One of the major issues of quaternion filtering techniques is the nonlinear group structure of the special orthogonal group SO(3). As unit quaternions are naturally located on the unit hypersphere $\mathbb{S}^3 \subset \mathbb{R}^4$, conventional filtering techniques, such as the Kalman filter (KF) and its derivatives, e.g., the extended Kalman filter (EKF) or unscented Kalman filter (UKF) (Van Der Merwe et al. (2001); Julier and Uhlmann (2004)), cannot be trivially applied. Adaptations were derived based on the local perturbation assumption (with Lie algebra for example) or by using high-order motion information (e.g., velocity or acceleration), such that conventional filters can be applied in a linearized/linear space (see Jahanchahi and Mandic (2014); Bloesch et al. (2017); Hauberg et al. (2013)).

Another branch of quaternion filters exploits distributions from directional statistics (Mardia and Jupp (2009)), such that uncertainty of unit quaternions can be modeled directly on the manifold without linearization. In this regard, the antipodal symmetry [1] of unit quaternions should be specifically considered. Therefore, the Bingham distribution on $\mathbb{S}^3$ has become a popular statistical tool for designing quaternion filters since the distribution is inherently antipodally symmetric. By assuming the Bingham distribution as the underlying noise distribution, Glover et al. (2012) have proposed Monte Carlo approaches for pose registration and further introduced quaternion filtering schemes based thereon (Glover and Kaelbling (2014)). There, quaternion samples are randomly drawn from the last Bingham posterior, propagated through the system model and then reweighted according to the measurement model for refitting the new posterior. To improve tracking efficiency, the deterministic sampling-based quaternion filter was proposed by Gilitschenski et al. (2016) following the concept of the unscented transform (seven samples are drawn to approximate moments up to the second order). Such an unscented quaternion filter still relies on identity measurement models, meaning the observation noise has to be Bingham-distributed. To eliminate this limitation, a progressive filtering scheme (see Hanebeck et al. (2003)) was employed by Li et al. (2018a) for handling general nonlinear quaternion estimation tasks (e.g., non-identity measurement model). To further improve nonlinear track-

⋆ This work is supported by the German Research Foundation (DFG) under grant HA 3789/16-1.

[1] The antipode of a unit quaternion represents the same orientation and thus should be endowed with identical density.

ing accuracy and robustness of the Bingham quaternion filtering, effort has also been dedicated to obtaining arbitrary numbers of deterministic samples that approximate higher-order shape information of the underlying density. By exploiting the hyperspherical geometry, Li et al. (2019a) enabled flexible deterministic sampling on the principal geodesic curves, which is further extended to the whole unit quaternion manifold in Li et al. (2019c). With more deterministic samples approximating higher-order shape information, nonlinearity of system dynamics can be better captured and improved tracking accuracy and robustness were shown.

The aforementioned works all rely on specific forms of the underlying distributions, regardless of whether the probability density function is employed on a locally linearized space or directly on the manifold. Such a parametric assumption can be error-prone for tracking scenarios with, e.g., multimodality, high nonlinearities, or non-stationarities, etc. The sequential Monte Carlo method, also known as particle filter (PF), allows complete modeling of arbitrary densities and has been deployed as filtering scheme in many nonlinear recursive estimation cases (see, e.g., Smith (2013)). Naively deploying PFs for nonlinear estimation tasks requires large numbers of particles and suffers from the curse of dimensionality (particularly for the four-dimensional quaternion particles). For peaky likelihoods or heavy-tailed noises, issues regarding efficient importance sampling should be specifically addressed. As was pointed out in Arulampalam et al. (2002), this mainly relates to the design of an effective proposal distribution. Adopting ideas of the UKF and the Gaussian particle filtering (see Kotecha and Djuric (2003)), Zhou et al. (2011) utilized a single quaternion-based UKF to obtain the proposal distribution. The samples are drawn from the UKF estimate for importance reweighting and the a posteriori density is updated thereafter. The approach has no resampling step and the Gaussianity assumption still plays a key role in it, resulting in a similar attitude tracking accuracy compared with the UKF. Van Der Merwe et al. (2001) first proposed the so-called unscented particle filter (UPF) with each particle running an individual UKF for obtaining its own proposal distribution within the PF scheme. Both theoretical proof and experimental results have shown superior tracking efficiency and accuracy, especially for highly nonlinear and non-stationary estimation tasks. However, existing works based on the UPF are still restricted to Euclidean spaces and no on-manifold extension has been made for nonlinear quaternion filtering.

In this work, we propose a novel hyperspherical unscented particle filter for recursive estimation of unit quaternions. Unlike other quaternion filtering approaches, it enables complete modeling of arbitrary densities on the manifold by exploiting the PF scheme. For improved handling of the nonlinearity with reasonable computational cost, a hyperspherical unscented Kalman filter is proposed based on the gnomonic projection/retraction for obtaining proposal distributions particle-wise for importance sampling. More specifically, the major contributions of this work are listed below.

- A quaternion particle filtering scheme is proposed without a parametric setup of the underlying density, enabling flexible and complete modeling of arbitrary uncertainties on the manifold.
- A novel unscented Kalman filter is proposed based on the gnomonic projection/retraction technique and deployed on each particle to obtain its individual proposal distribution for importance sampling.
- The proposed quaternion filtering approach is applied to nonlinear orientation estimation. Simulation results show improved tracking accuracy compared with existing quaternion filters.

The remainder of the paper is structured as follows. In Sec. 2, preliminaries about quaternion arithmetics and the particle filter are introduced. The geometric structure of the unit quaternion manifold with consideration of on-manifold stochastic modeling is introduced in Sec. 3. The novel quaternion unscented particle filtering scheme is proposed in Sec. 4 and evaluated in Sec. 5. Finally, the work is concluded in Sec. 6.

2. PRELIMINARIES

By convention, an axis-angle representation of a spatial rotation can be parameterized by a quaternion in the following vector form

$$\mathbf{x} = [\,\cos(\theta/2),\, \sin(\theta/2)\,\mathbf{n}^\top\,]^\top := [\,x_0,\, x_1,\, x_2,\, x_3\,]^\top, \quad (1)$$

with θ being the rotation angle and the unit vector $\mathbf{n}$ the rotation axis. Given a unit quaternion of the form above, any point $\mathbf{v} \in \mathbb{R}^3$ can be rotated according to

$$\mathbf{v}' = \left(\mathbf{x} \otimes [\,0,\, \mathbf{v}^\top\,]^\top \otimes \mathbf{x}^*\right)_{2:4}. \quad (2)$$

Here, $\mathbf{x}^* = \mathrm{diag}(1,-1,-1,-1)\,\mathbf{x}$ denotes the conjugate of $\mathbf{x}$ and $\otimes$ is the Hamilton product. We take out the last three elements of the rotated quaterinon (the first element is zero) to reobtain the rotated vector. Given a quaternion $\mathbf{x}$, its norm is defined as $\|\mathbf{x}\| = \mathbf{x} \otimes \mathbf{x}^*$. Therefore, quaternions representing spatial rotations in (1) are of unit norm and are called unit quaternions. The Hamilton product $\otimes$ aggregates two quaternions and can be re-parameterized into an ordinary matrix–vector multiplication. For instance, $\mathbf{x} \otimes \mathbf{y} = \mathcal{Q}^{\llcorner}_{\mathbf{x}}\,\mathbf{y} = \mathcal{Q}^{\lrcorner}_{\mathbf{y}}\,\mathbf{x}$ with

$$\mathcal{Q}^{\llcorner}_{\mathbf{x}} = \begin{bmatrix} x_0 & -x_1 & -x_2 & -x_3 \\ x_1 & x_0 & -x_3 & x_2 \\ x_2 & x_3 & x_0 & -x_1 \\ x_3 & -x_2 & x_1 & x_0 \end{bmatrix},\ \mathcal{Q}^{\lrcorner}_{\mathbf{y}} = \begin{bmatrix} y_0 & -y_1 & -y_2 & -y_3 \\ y_1 & y_0 & y_3 & -y_2 \\ y_2 & -y_3 & y_0 & y_1 \\ y_3 & y_2 & -y_1 & y_0 \end{bmatrix}. \quad (3)$$

As unit quaternions are also of unit length in the Euclidean space, the unit hypersphere $\mathbb{S}^3 \subset \mathbb{R}^4$ is a double covering of the SO(3) group, which is closed under the Hamilton product. Given a unit quaternion $\mathbf{x} \in \mathbb{S}^3$, it can be easily verified that matrices in (3) satisfy $\mathcal{Q}^{\lrcorner\top}_{\mathbf{x}}\mathcal{Q}^{\lrcorner}_{\mathbf{x}} = \mathcal{Q}^{\lrcorner}_{\mathbf{x}}\mathcal{Q}^{\lrcorner\top}_{\mathbf{x}} = \mathbf{I}_{4\times 4}$ and $\det(\mathcal{Q}^{\lrcorner}_{\mathbf{x}}) = 1$ (also valid for the left matrix $\mathcal{Q}^{\llcorner}_{\mathbf{x}}$). Thus, the matrix representation of unit quaternions belongs to the four-dimensional rotational group $\mathrm{SO}(4)$. Furthermore, the inverse of a unit quaternion corresponds to the transpose of its matrix form, for instance $\mathcal{Q}^{\lrcorner}_{\mathbf{x}^{-1}} = \mathcal{Q}^{\lrcorner\top}_{\mathbf{x}}$, indicating an inverse rotation on $\mathbb{S}^3$ geometrically.

2.1 Sequential Monte Carlo Methods of Unit Quaternions

We focus on nonlinear quaternion estimation problems with the system model as follows

$$\mathbf{x}_k = a(\mathbf{x}_{k-1}, \mathbf{w}_{k-1}), \quad (4)$$

where $\mathbf{x}_{k-1}, \mathbf{x}_k \in \mathbb{S}^3$ are the unit quaternion states, $\mathbf{w}_{k-1} \in \mathbb{W}$ the system noise and $a : \mathbb{S}^3 \times \mathbb{W} \to \mathbb{S}^3$ the transition function. The measurement model is given as

$$\mathbf{z}_k = h(\mathbf{x}_k, \mathbf{v}_k)\,, \tag{5}$$

with $\mathbf{z}_k \in \mathbb{Z}$ denoting the measurement, $\mathbf{v}_k \in \mathbb{V}$ the measurement noise and $h : \mathbb{S}^3 \times \mathbb{V} \to \mathbb{Z}$ the observation function. The sequential Monte Carlo method, i.e., the particle filter, models the posterior distribution by means of Dirac mixtures located at each particle $\boldsymbol{\mu}_k^i$, i.e.,

$$p(\mathbf{x}_{0:k}|\mathbf{z}_{1:k}) = \textstyle\sum_{i=1}^{n} \omega_k^i\, \delta(\mathbf{x}_{0:k} - \boldsymbol{\mu}_k^i)\,, \tag{6}$$

with $\delta(\cdot)$ being the Dirac delta function and ω_k^i the weights ($\sum_{i=1}^{n} \omega_k^i = 1$). However, it is theoretically infeasible to draw samples directly from the posterior density $p(\mathbf{x}_{0:k}|\mathbf{z}_{1:k})$. Instead, i.i.d. samples are drawn from a known and easy-to-sample distribution, namely the proposal distribution $q(\mathbf{x}_k|\mathbf{x}_{0:k-1}, \mathbf{z}_{1:k})$, such that importance weights can be evaluated recursively according to

$$\omega_k^i = \omega_{k-1}^i \frac{p_{\mathrm{L}}(\mathbf{z}_k|\mathbf{x}_k^i)\, p(\mathbf{x}_k^i|\mathbf{x}_{k-1}^i)}{q(\mathbf{x}_k^i|\mathbf{x}_{0:k-1}^i, \mathbf{z}_{1:k})}\,. \tag{7}$$

Here, $p_{\mathrm{L}}(\mathbf{z}_k|\mathbf{x}_k^i)$ denotes the likelihood evaluated at each particle $\mathbf{x}_k^i$ given measurement $\mathbf{z}_k$. After that, weights are normalized, based on which a resampling is performed (e.g., by using inverse transform sampling). A detailed introduction to basic particle filtering can be found in Arulampalam et al. (2002).

As shown in (7), designing and estimating the proposal distribution appropriately plays an important role for the performance of the particle filter. More specifically, one possible proposal distribution of a quaternion particle filter is the transition density that can be easily derived from the system model in (4). However, setting $q(\mathbf{x}_k|\mathbf{x}_{0:k-1}, \mathbf{z}_{1:k}) = p(\mathbf{x}_k|\mathbf{x}_{k-1})$ disregards the recently coming information, i.e., the measurement. Inspired by the work done by Van Der Merwe et al. (2001), we propose to apply the UKF on the hypersphere to evaluate the proposal density for each quaternion particle. The resulting hyperspherical unscented particle filter (HUPF) enables incorporating recently observed evidence and can drive the particles to high-likelihood regions on the manifold. As a result, PF-based quaternion estimations can be improved especially in the cases where, e.g., heavy-tailed state densities, non-stationary model or peaky likelihood, exist.

3. GEOMETRIC STRUCTURE OF UNIT QUATERNION MANIFOLD

One of the key components of the aforementioned quaternion unscented particle filter is the adaptation to the manifold structure. Conventional UKFs can only be deployed in the Euclidean space as the noise term is assumed to be Gaussian-distributed. Distributions from directional statistics such as the Bingham distribution, the von Mises–Fischer distribution or the projected Gaussian distribution by Feiten et al. (2013), do allow stochastic modeling of uncertain unit quaternions on the manifold $\mathbb{S}^3$ and unscented transform-based directional estimation approaches exist (Gilitschenski et al. (2016)). However, efficiency issues arise when deploying directional estimators in the HUPF scheme. First, fitting a hyperspherical Bingham or von Mises–Fisher density from samples requires time-consuming calculation of normalization constants since no closed-form solution exists. Though accelerations or look-up tables have been introduced (e.g., in Gilitschenski et al. (2014); Glover and Kaelbling (2014)), the computational burden cannot be alleviated substantially for particle-wise operations. Second, directional estimation approaches rely on a large number of deterministic samples (generated via online optimization) or the progressive filtering scheme for nonlinear estimation, which worsen computational efficiency as well.

On the other hand, there exist works adapting the UKF on Riemannian manifolds, as proposed in Hauberg et al. (2013); Menegaz et al. (2019). Here, the key idea is to estimate an on-tangent-plane Gaussian distribution in the UKF scheme via the logarithm/exponential map. The set of unit quaternions forms a compact Riemannian manifold with a spherical structure. Any point $\mathbf{x} \in \mathbb{S}^3$ can be mapped to the tangent plane at a given point $\boldsymbol{\mu} \in \mathbb{S}^3$, denoted as $\mathbb{T}_{\boldsymbol{\mu}}\mathbb{S}^3$, via the logarithm map

$$\mathbf{x}_{\mathrm{t}} = \mathrm{Log}_{\boldsymbol{\mu}}(\mathbf{x}) = (\mathbf{x} - \cos(\beta)\,\boldsymbol{\mu})\,\beta/\sin(\beta) \in \mathbb{T}_{\boldsymbol{\mu}}\mathbb{S}^3\,,$$

with $\beta = \mathrm{acos}(\mathbf{x}^\top \boldsymbol{\mu})$ being the arc length between $\mathbf{x}$ and $\boldsymbol{\mu}$. The inverse operation, namely the exponential map, is

$$\mathbf{x} = \mathrm{Exp}_{\boldsymbol{\mu}}(\mathbf{x}_{\mathrm{t}}) = \cos(\|\mathbf{x}_{\mathrm{t}}\|)\,\boldsymbol{\mu} + \mathbf{x}_{\mathrm{t}} \sin(\|\mathbf{x}_{\mathrm{t}}\|)\,/\|\mathbf{x}_{\mathrm{t}}\| \in \mathbb{S}^3\,.$$

Unscented transform on manifolds often deploys a zero-mean Gaussian distribution on the tangent plane, from which the sigma points are drawn. The samples can then be mapped to the manifold via the exponential map and diffused through uncertain system dynamics or updated by the likelihood on the manifold, such that the on-tangent-plane Gaussian distribution can be estimated again via the logarithm map. It can be easily verified that the exponential and logarithm map preserve the geodesic length in respective domains, i.e., $\|\mathrm{Log}_{\boldsymbol{\mu}}(\mathbf{x})\| = \beta \in [0, \pi/2]$ (consider antipodal symmetry). The tangent plane at an arbitrary point on the unit quaternion manifold is therefore a bounded Euclidean space. As the support of the Gaussian distribution is unbounded, such a set-up is not theoretically sound and may trigger robustness problems, especially in the case of large uncertainties or non-zero-mean noise. Sigma points can be drawn in these cases outside the range limit $\pi/2$ and miss-interpret the uncertainty after being mapped to the manifold via exponential map.

From the perspective of Riemannian optimization (see Absil et al. (2009); Absil and Malick (2012)), we propose to use the gnomonic projection/retraction as the geometric tool for interpreting the uncertainty of unit quaternions on the tangent plane (see also Li et al. (2019a,c) for details). The gnomonic projection shoots a ray from the sphere center through a given point $\mathbf{x} \in \mathbb{S}^3$ and find its intersection $\mathbf{x}_{\mathrm{t}}$ on a given tangent plane at $\boldsymbol{\mu} \in \mathbb{S}^3$. Mathematically, the gnomonic projection is expressed as

$$\mathbf{x}_{\mathrm{t}} = \mathcal{P}_{\boldsymbol{\mu}}(\mathbf{x}) = \mathbf{x}/(\boldsymbol{\mu}^\top \mathbf{x}) \in \mathbb{T}_{\boldsymbol{\mu}}\mathbb{S}^3\,, \forall \mathbf{x} \in \mathbb{S}^3\,,$$

with $\mathbb{T}_{\boldsymbol{\mu}}\mathbb{S}^3$ denoting the tangent plane at $\boldsymbol{\mu}$. The inverse mapping, namely the gnomonic retraction, is essentially the normalization of on-tangent-plane points, i.e.,

$$\mathbf{x} = \mathcal{R}_{\boldsymbol{\mu}}(\mathbf{x}_{\mathrm{t}}) = \mathbf{x}_{\mathrm{t}}/\|\mathbf{x}_{\mathrm{t}}\|\,, \forall \mathbf{x}_{\mathrm{t}} \in \mathbb{T}_{\boldsymbol{\mu}}\mathbb{S}^3\,.$$

As introduced in Sec. 2, the Hamilton product for unit quaternions can be geometrically interpreted as four-dimensional rotation applied to $\mathbb{S}^3$. Therefore, following relations can be established when performing the

gnomonic projection/retraction between arbitrary unit quaternions and the identity quaternion $\mathbb{1} = [1, 0, 0, 0]^\top$.

$$\mathcal{R}_{\boldsymbol{\mu}}(\mathbf{x}_\mathrm{t}) = \boldsymbol{\mu} \otimes \mathcal{R}_{\mathbb{1}}(\boldsymbol{\mu}^{-1} \otimes \mathbf{x}_\mathrm{t}) \in \mathbb{S}^3, \forall \mathbf{x}_\mathrm{t} \in \mathbb{T}_{\boldsymbol{\mu}}\mathbb{S}^3\,,$$
$$\mathcal{P}_{\boldsymbol{\mu}}(\mathbf{x}) = \boldsymbol{\mu} \otimes \mathcal{P}_{\mathbb{1}}(\boldsymbol{\mu}^{-1} \otimes \mathbf{x}) \in \mathbb{T}_{\boldsymbol{\mu}}\mathbb{S}^3, \forall \mathbf{x} \in \mathbb{S}^3\,,$$

which denote the rotation via $\boldsymbol{\mu}^{-1}$ followed by the desired operation (retraction or projection) at the identity and the back-rotation to $\boldsymbol{\mu}$ thereafter.

Under the gnomonic projection, a Gaussian distribution on the tangent plane is free from range limitation when interpreting the uncertainty of quaternions on the sphere. Also, stochastic modeling of antipodal symmetry is inherently guaranteed, since an infinitely remote point on the tangent plane is projected onto inside of the corresponding hemisphere (asymptotically on the sphere equator). The tangent plane of the unit quaternion manifold is the four-dimensional Euclidean space with three DoF (as it is tangential to the sphere at $\boldsymbol{\mu}$). For setting up the particle-wise UKF, a three-dimensional zero-mean Gaussian distribution is therefore deployed w.r.t. a local coordinate of the tangent plane at each quaternion particle. As shown in (3), the matrix representation of a unit quaternion $\mathbf{x}$ naturally entails the orthonormal basis for referencing the tangent space at $\mathbf{x}$. For instance, when denoting the matrix-form quaternion columnwise as $\mathcal{Q}^{\mathsf{L}}_{\mathbf{x}} = [\mathbf{x}, \mathbf{e}_1, \mathbf{e}_2, \mathbf{e}_3]$, the last three column vectors expand the tangent space at $\mathbf{x}$, namely $\mathbb{T}_{\mathbf{x}}\mathbb{S}^3 = \mathrm{span}\{\mathbf{e}_1, \mathbf{e}_2, \mathbf{e}_3\}$. Therefore, points on specific tangent planes can be transformed to orientation-invariant coordinates in $\mathbb{R}^3$. Thus, the gnomonic projection/retraction w.r.t. the local basis can be derived as

$$\boldsymbol{\tau} = \big((\mathcal{P}_{\mathbb{1}}(\boldsymbol{\mu}^{-1} \otimes \mathbf{x}) - \mathbb{1})\big)_{2:4} \in \mathbb{R}^3, \forall \mathbf{x} \in \mathbb{S}^3\,, \tag{8}$$

$$\mathbf{x} = \boldsymbol{\mu} \otimes \mathcal{R}_{\mathbb{1}}(\mathbb{1} + [0, \boldsymbol{\tau}^\top]^\top) \in \mathbb{S}^3, \forall \boldsymbol{\tau} \in \mathbb{R}^3\,. \tag{9}$$

In this manner, the on-tangent-plane UKF of each particle is then invariant to its location on the manifold.

4. HYPERSPHERICAL UNSCENTED PARTICLE FILTERING

In the proposed HUPF, each quaternion particle $\boldsymbol{\mu}^i_k \in \mathbb{S}^3$ in (6) is augmented as $(\boldsymbol{\mu}^i_k, \omega^i_k, \mathbf{C}^i_k)$ with its weight ω^i_k and a covariance matrix $\mathbf{C}^i_k \in \mathbb{R}^{3\times3}$. A zero-mean Gaussian distribution $\mathcal{N}(\mathbf{0}, \mathbf{C}^i_k)$ is deployed under the gnomonic projection on the tangent plane at $\boldsymbol{\mu}^i_k$ w.r.t. its local basis for depicting the uncertainty of each individual particle. The UKF in Wan and Van Der Merwe (2000) is modified according to the hyperspherical geometry to obtain the posterior estimate of $\boldsymbol{\mu}^i_k$ and $\mathbf{C}^i_k$ as the proposal for importance sampling.

The quaternion particles are initialized via random sampling of the initial posterior density $p(\mathbf{x}_0|\mathbf{z}_0)$ that is assumed to be $p(\mathbf{x}_0)$. The detailed procedure of each recursive estimation step is shown in Alg. 1. Given the last posterior estimate of the particle $\boldsymbol{\mu}^i_{k-1}$ and covariance $\mathbf{C}^i_{k-1}$, sigma points $\{\boldsymbol{\tau}^{i,s}_{k-1}\}^m_{s=1}$ are first drawn on the tangent plane w.r.t. its local basis with weights ν_s. The local sigma points are then retracted to the manifold and transformed into global coordinates. Here, function $\texttt{retract}(\mathbf{a}, \mathbf{b})$ maps points $\mathbf{b}$ w.r.t. the local basis on $\mathbb{T}_{\mathbf{a}}\mathbb{S}^3$ to quaternions of global coordinates via the gnomonic retraction in (9). Afterward, the quaternion sigma points

Algorithm 1: HUPF

Input: $\{(\boldsymbol{\mu}^i_{k-1}, \omega^i_{k-1}, \mathbf{C}^i_{k-1})\}^n_{i=1}$, measurement $\mathbf{z}_k$
Output: $\{(\boldsymbol{\mu}^i_k, \omega^i_k, \mathbf{C}^i_k)\}^n_{i=1}$

```
/* particle-wise UKF on S^3                                          */
for i ← 1 to n do
    /* UKF prediction                                                */
    {(τ^{i,s}_{k-1}, ν_s)}^m_{s=1} ← getSigmaPoints(C^i_{k-1});
    {χ^{i,s}_{k-1}}^m_{s=1} ← retract(μ^i_{k-1}, {τ^{i,s}_{k-1}}^m_{s=1});   // (9)
    {χ^{i,s}_{k|k-1}}^m_{s=1} ← propagate({χ^{i,s}_{k-1}}^m_{s=1});          // (4)
    μ̄^i_{k|k-1} ← average({(χ^{i,s}_{k|k-1}, ν_s)}^m_{s=1});
    {τ^{i,s}_{k|k-1}}^m_{s=1} ← proj(μ̄^i_{k|k-1}, {χ^{i,s}_{k|k-1}}^m_{s=1});  // (8)
    C^i_{k|k-1} ← Σ_s ν_s τ^{i,s}_{k|k-1} (τ^{i,s}_{k|k-1})^⊤;
    {z^{i,s}_{k|k-1}}^m_{s=1} ← measure({χ^{i,s}_{k|k-1}}^m_{s=1});          // (5)
    /* UKF update                                                    */
    z̄^i_{k|k-1} ← Σ_s z^{i,s}_{k|k-1};
    C^i_z ← Σ_s ν_s (z^{i,s}_{k|k-1} − z̄^i_{k|k-1})(z^{i,s}_{k|k-1} − z̄^i_{k|k-1})^⊤;
    C^i_{τz} ← Σ_s ν_s τ^{i,s}_{k|k-1} (z^{i,s}_{k|k-1} − z̄^i_{k|k-1})^⊤;
    K^i_k ← C^i_{τz} (C^i_z)^{-1};
    τ̄^i_k ← K^i_k (z_k − z̄^i_{k|k-1});
    C^i_k ← C^i_{k|k-1} − K^i_k C^z_i (K^i_k)^⊤;
    μ̄^i_k ← retract(μ̄^i_{k|k-1}, τ̄^i_k);                                  // (9)
    /* particle-wise reweighting                                     */
    τ̂^i_k ← getRndSample(N(0, C^i_k));
    x̂^i_k ← retract(μ̄^i_k, τ̂^i_k);                                        // (9)
    ω^i_k ← ω^i_{k-1} f(z_k|x̂^i_k) f(x̂^i_k|x^i_{k-1}) / f(x̂^i_k|x^i_{0:k-1}, z_{1:k});   // (7)
end
{ω̃^i_k}^n_{i=1} ← normalize({ω^i_k}^n_{i=1});
{(μ^i_k, ω^i_k, C^i_k)}^n_{i=1} ← resample({(μ̄^i_k, ω̃^i_k, C^i_k)}^n_{i=1});
return {(μ^i_k, ω^i_k, C^i_k)}^n_{i=1}
```

$\{\boldsymbol{\chi}^{i,s}_{k-1}\}^m_{s=1}$ are propagated through the system dynamics according to (4). The prior mean $\bar{\boldsymbol{\mu}}^i_{k|k-1}$ is then computed using the intrinsic gradient descent algorithm as suggested by Kraft (2003)[2]. Afterward, the propagated quaternion sigma points $\{\boldsymbol{\chi}^{i,s}_{k|k-1}\}^m_{s=1}$ are mapped by function `proj` to the shifted tangent plane at $\bar{\boldsymbol{\mu}}^i_{k|k-1}$ w.r.t. its local basis according to (8) and the prior covariance $\mathbf{C}^i_{k|k-1}$ is computed. Meanwhile, the predicted measurements for the sigma points are obtained according to the measurement model in (5). Then, we fuse the measurement $\mathbf{z}_k$ on the prior tangent plane at $\bar{\boldsymbol{\mu}}^i_{k|k-1}$ to obtain the posterior mean $\bar{\boldsymbol{\tau}}^i_k$ in the local basis. Consequently, the location of tangent plane is updated to $\bar{\boldsymbol{\mu}}^i_k$, around which the posterior Gaussian distribution of covariance $\mathbf{C}^i_k$ is centralized. Given the on-tangent-plane UKF proposal above, importance sampling is then performed. An individual particle $\hat{\mathbf{x}}^i_k$ is generated by randomly sampling from corresponding posterior estimate $\mathcal{N}(\mathbf{0}, \mathbf{C}^i_k)$ w.r.t. the local basis at $\bar{\boldsymbol{\mu}}^i_k$ and retracting to $\mathbb{S}^3$ thereafter. Subsequently, the particle weights are updated according to (7) and re-normalized. For handling potential degeneration issues, one can apply

[2] Corresponding to the proposed noise model, we measure the error metric on tangent plane under the gnomonic projection.

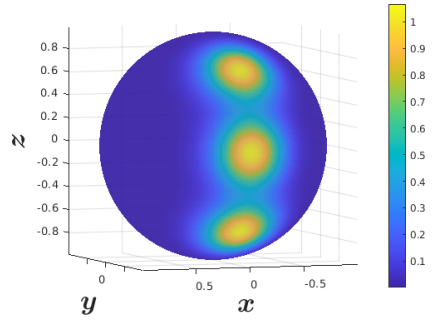

Fig. 1. Multimodal distribution of uncertain rotation axis used in Sec. 5.2. It is synthesized by a von Mises–Fisher mixture with $\kappa = 20$ for each component.

the resampling approaches in Arulampalam et al. (2002) to obtain uniformly weighted particles.

5. EVALUATION

We evaluate the proposed hyperspherical unscented particle filter for nonlinear quaternion estimation based on simulations. The system model is set up as

$$\mathbf{x}_k = \mathbf{x}_{k-1} \otimes \mathbf{w}_{k-1}^2 \,, \tag{10}$$

containing a squared random system input $\mathbf{w}_k^2 \triangleq \mathbf{w}_k \otimes \mathbf{w}_k$ with $\mathbf{w}_k = [\cos(0.5\,\theta_\mathrm{w}), \boldsymbol{\zeta}_\mathrm{w}^\top \sin(0.5\,\theta_\mathrm{w})]^\top \in \mathbb{S}^3$. The randomness is hereby introduced by the rotation angle θ_w and the rotation axis $\boldsymbol{\zeta}_\mathrm{w}$, which are assumed to follow different distributions in the individual test cases. Furthermore, we apply the following measurement model

$$\mathbf{z}_k = \left(\mathbf{x}_k \otimes [0, \mathbf{s}_0^\top]^\top \otimes \mathbf{x}_k\right)_{2:4} + \mathbf{v}_k \,,$$

which rotates a point initialized at $\mathbf{s}_0$ according to the current quaternion state as introduced in (2). An additive measurement noise is applied after the position observation and assumed to follow a zero-mean Gaussian distribution, i.e., $\mathbf{v}_k \sim \mathcal{N}(\mathbf{0}, \boldsymbol{\Sigma}_\mathrm{v})$. Thus, it is straightforward to derive the likelihood function in (7) as

$$f(\mathbf{z}_k|\mathbf{x}_k) = f_\mathrm{v}\Big(\mathbf{z}_k - \left(\mathbf{x}_k \otimes [0, \mathbf{s}_0^\top]^\top \otimes \mathbf{x}_k\right)_{2:4}\Big) \,.$$

For evaluating the tracking accuracy in an intuitive way, we map the estimated quaternion states $\hat{\mathbf{x}}_k$ to the measurement space via the observation equation $(\hat{\mathbf{x}}_k \otimes [0, \mathbf{s}_0^\top]^\top \otimes \hat{\mathbf{x}}_k)_{2:4}$ and compare it with the one given by the ground truth. Such a conversion does not conceal error as it keeps the degree of freedom unchanged. Thus, the estimation error can be expressed as the Euclidean distance. For all the evaluation cases below, we perform 100 Monte Carlo runs of 50 steps and plot the error as well as runtime statistics with box plots [3].

5.1 Evaluation under Different Measurement Noise Levels

In this test case, we apply the proposed HUPF for the given orientation estimation problem under different measurement noise levels of $\boldsymbol{\Sigma}_\mathrm{v} = c \cdot \mathbf{I}_{3\times3}$, with $c \in \{0.1, 0.05, 0.0005\}$ and $\mathbf{I}_{3\times3} \in \mathbb{R}^{3\times3}$ being the identity matrix. For the random system input $\mathbf{w}_{k-1}$ as defined in (10), the uncertain angular term θ_w is assumed to be von Mises-distributed and the axis term $\boldsymbol{\zeta}_\mathrm{w}$ follows a von Mises–Fisher distribution, i.e., $\theta_\mathrm{w} \sim \mathcal{VM}(\phi_\mathrm{w}^\theta, \kappa_\mathrm{w}^\theta)$ and $\boldsymbol{\zeta}_\mathrm{w} \sim \mathcal{VMF}(\boldsymbol{\phi}_\mathrm{w}^\zeta, \kappa_\mathrm{w}^\zeta)$, respectively. The mean values for rotation angle and axis are $\phi_\mathrm{w}^\theta = \pi/6$, $\boldsymbol{\phi}_\mathrm{w}^\zeta = [1\sqrt{3}, 1\sqrt{3}, 1\sqrt{3}]^\top$, and $\kappa_\mathrm{w}^\theta = \kappa_\mathrm{w}^\zeta = 100$ denote their uncertainties, with smaller value indicating stronger noise. As comparisons, we run the conventional quaternion particle filter using 2000 samples with the same resampling scheme and two other existing quaternion filters using the Bingham distributions, which rely on a parametric modeling of the underlying density. Considering the nonlinearity, we deploy the unscented Bingham filter by Gilitschenski et al. (2016) (drawing 7 deterministic samples) within the progressive filtering scheme in Hanebeck et al. (2003) (ProgUKF-7). Furthermore, a Bingham filter (RieBF-200) using 200 deterministic samples generated by the Riemannian spherical sampling approach proposed in Li et al. (2019c) is used.

As shown in Fig. 2, the proposed filter shows superior performance regarding accuracy and runtime compared with the other nonlinear quaternion filters under high and medium measurement noise levels. The ProgUBF has the same prediction step as proposed in Gilitschenski et al. (2016) [4] and updates the prior progressively adaptive to the likelihood difference among the samples when fusing the measurement. When an increased nonlinearity appears in the measurement model, the ProgUKF can obtain good accuracy, however, with a sacrifice on computational efficiency due to the progressive scheme. The proposed HUPF shows particularly good robustness under low noise level, where all the other filters lose tracking due to the nonlinear motion model and the peaky likelihood function. In this case, approaches based on parametric representations of the state uncertainty, i.e., the ProgUBF and the RieBF, prominently suffer from sample degeneration. The conventional particle filter, though deploying much more particles than the HUBF, also fails because its proposal distribution disregards the recent observation as discussed in Sec. 2.1.

5.2 Evaluation under Multimodal Uncertainty

We further set the uncertain rotation axis of the system input $\mathbf{w}_k$ to follow a multimodal distribution synthesized by the mixture of von Mises–Fisher distributions on $\mathbb{S}^2$ (shown in Fig. 1). The system model is the same as in (10) and the measurement noise level is fixed to be the medium one, i.e., $\boldsymbol{\Sigma}_\mathrm{v} = 0.05 \times \mathbf{I}_{3\times3}$. Fig. 3 shows the comparative evaluation result with competitive filters of enhanced configurations. Here, the sample size of the RieBF is raised to be 500 and the conventional PF deploys 4000 particles. Due to the nonlinearity and the multimodality, only the proposed HUPF gives functional tracking performance. Furthermore, increasing the number of particles of the HUPF gives improved tracking accuracy with more computational cost, as shown in Fig. 3 (b)-(c). For illustrating the functionality of the HUPF in this test case, another system noise is synthesized in the same way as shown in Fig. 1, however, with a decreased uncertainty of $\kappa_\mathrm{w}^\theta = 500$ and $\kappa = 500$ for each of the three von Mises–Fisher components. Meanwhile, the number of particles of the PF is increased to 6000. The number of particles for the HUPF is kept as 50. As shown in Fig. 4, samples

[3] In tracking failure cases, error and runtime are set to be zero on purpose as shown, e.g., in Fig. 2(c) and Fig. 3(a).

[4] As the system model here restricts the noise term to be Bingham-distributed, 5×10^5 samples are used for approximating the desired Bingham system noise distribution.

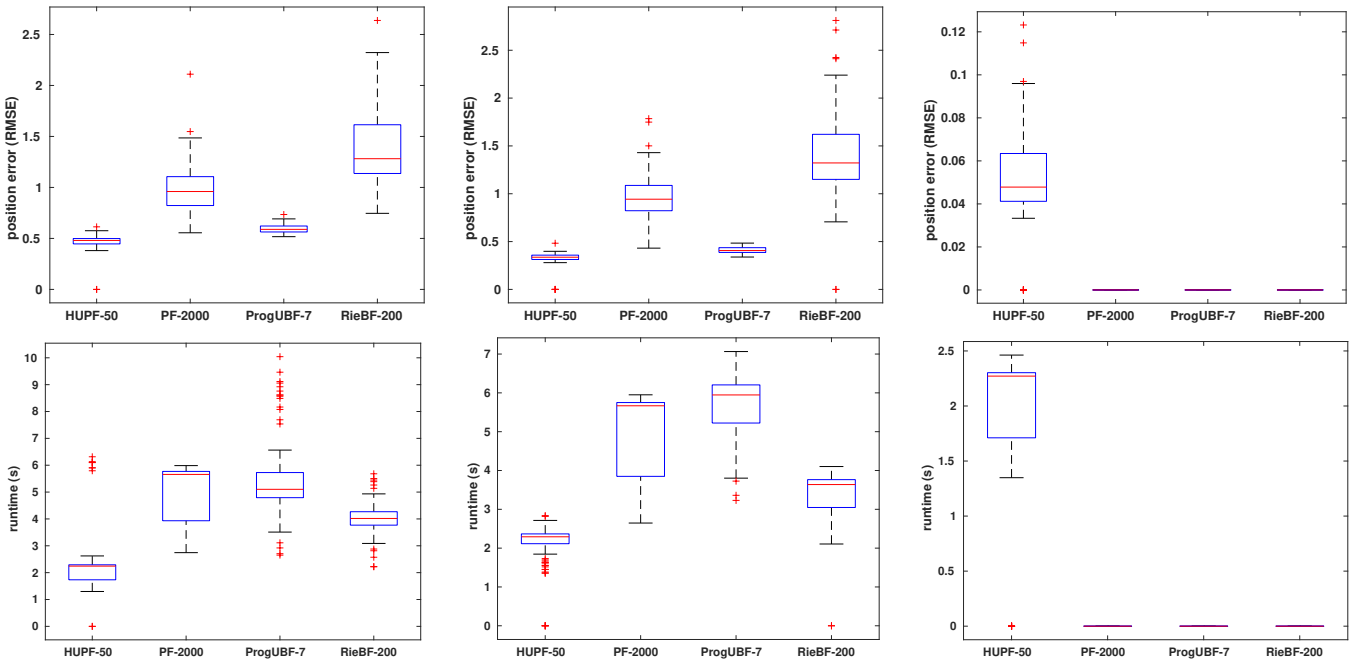

(a) large noise (b) medium noise (c) low noise

Fig. 2. Comparison of the HUPF with existing quaternion filters. The proposed HUPF outperforms the others regarding accuracy, efficiency, and robustness for large and medium noise.

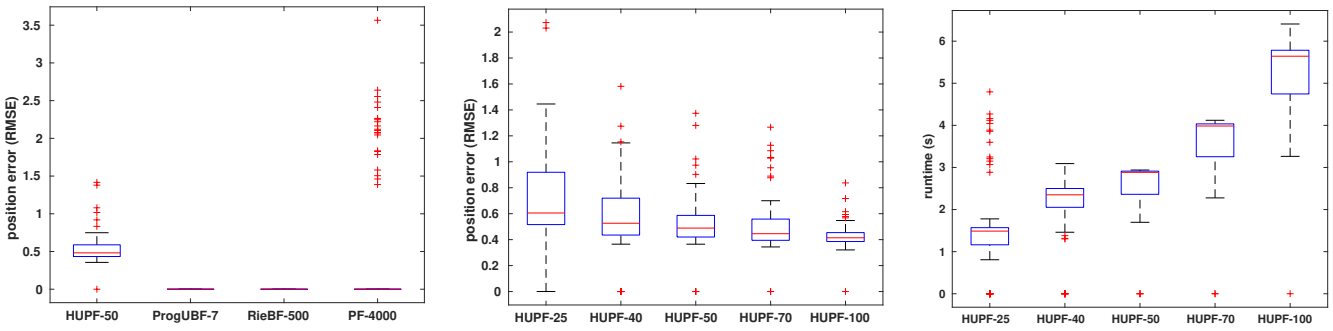

(a) comparative results (b) accuracy (c) runtime

Fig. 3. Evaluation on nonlinear quaternion estimation with multimodal noise. The tracking accuracy of the HUPF is improved when increasing the number of particles, which causes higher computational costs.

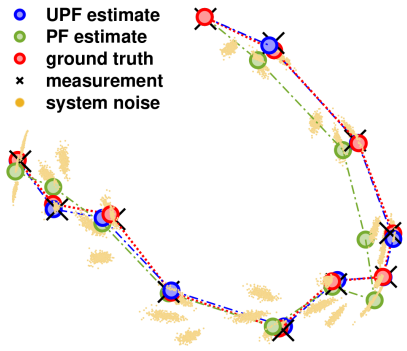

Fig. 4. Demonstration of tracking under multimodal noise.

(yellow dots) from the multimodal system noise are drawn and propagated in every step. Compared with the conventional particle filtering scheme, the HUPF is designed to incorporate the current observation and move particles to the high-likelihood regions, thus giving better tracking accuracy in a much more efficient manner.

6. CONCLUSION

We proposed a novel stochastic filtering approach for nonlinear quaternion estimation. By applying the unscented particle filtering scheme, no parametric assumption of the underlying distribution is required and recent observations are considered for importance sampling. To handle the nonlinear structure of the unit quaternion manifold, we investigated the hyperspherical geometry to deploy the UKF on the tangent plane w.r.t. to its local basis for obtaining particle-wise proposal distributions. The resulting hyperspherical unscented particle filter has been observed to evidently improve performance and flexibility for nonlinear quaternion estimation. There is still much potential to exploit on basis of this work. For instance, the HUPF can be extended for recursive estimation of 6-DoF poses within a proper probabilistic inference framework (Li et al. (2018b, 2019b)). Further, it is appealing to investigate its performance in real-world scenarios, such as point registration and visual odometry (Bultmann et al. (2019)).

REFERENCES

Absil, P.A., Mahony, R., and Sepulchre, R. (2009). *Optimization Algorithms on Matrix Manifolds*. Princeton University Press.

Absil, P.A. and Malick, J. (2012). Projection-like Retractions on Matrix Manifolds. *SIAM Journal on Optimization*, 22(1), 135–158.

Arulampalam, M.S., Maskell, S., Gordon, N., and Clapp, T. (2002). A Tutorial on Particle Filters for Online Nonlinear/non-Gaussian Bayesian Tracking. *IEEE Transactions on signal processing*, 50(2), 174–188.

Bloesch, M., Burri, M., Omari, S., Hutter, M., and Siegwart, R. (2017). Iterated Extended Kalman Filter Based Visual-Inertial Odometry Using Direct Photometric Feedback. *The International Journal of Robotics Research*, 36(10), 1053–1072.

Bultmann, S., Li, K., and Hanebeck, U.D. (2019). Stereo Visual SLAM Based on Unscented Dual Quaternion Filtering. In *Proceedings of the 22nd International Conference on Information Fusion (Fusion 2019)*. Ottawa, Canada.

Feiten, W., Lang, M., and Hirche, S. (2013). Rigid Motion Estimation Using Mixtures of Projected Gaussians. In *Proceedings of the 16th International Conference on Information Fusion*, 1465–1472. IEEE.

Gilitschenski, I., Kurz, G., Julier, S.J., and Hanebeck, U.D. (2014). Efficient Bingham Filtering based on Saddlepoint Approximations. In *Proceedings of the 2014 IEEE International Conference on Multisensor Fusion and Information Integration (MFI 2014)*. Beijing, China.

Gilitschenski, I., Kurz, G., Julier, S.J., and Hanebeck, U.D. (2016). Unscented Orientation Estimation Based on the Bingham Distribution. *IEEE Transactions on Automatic Control*, 61(1), 172–177.

Glover, J., Bradksi, G., and Rusu, R. (2012). Monte Carlo Pose Estimation with Quaternion Kernels and the Bingham Distribution. In *Proceedings of Robotics: Science and Systems*. Los Angeles, CA, USA.

Glover, J. and Kaelbling, L.P. (2014). Tracking the Spin on a Ping Pong Ball with the Quaternion Bingham Filter. In *2014 IEEE International Conference on Robotics and Automation (ICRA 2014)*, 4133–4140.

Hanebeck, U.D., Briechle, K., and Rauh, A. (2003). Progressive Bayes: A New Framework for Nonlinear State Estimation. In *Proceedings of SPIE, AeroSense Symposium*, volume 5099, 256 – 267. Orlando, Florida, USA.

Hashim, H.A., Brown, L.J., and McIsaac, K.A. (2019). Guaranteed Performance of Nonlinear Attitude Filters on the Special Orthogonal Group SO(3). *IEEE Access*, 7, 3731–3745.

Hauberg, S., Lauze, F., and Pedersen, K.S. (2013). Unscented Kalman Filtering on Riemannian Manifolds. *Journal of Mathematical Imaging and Vision*, 46(1), 103–120.

Jahanchahi, C. and Mandic, D.P. (2014). A Class of Quaternion Kalman Filters. *IEEE Transactions on Neural Networks and Learning Systems*, 25(3), 533–544.

Julier, S.J. and Uhlmann, J.K. (2004). Unscented Filtering and Nonlinear Estimation. *Proceedings of the IEEE*, 92(3), 401–422.

Kotecha, J.H. and Djuric, P.M. (2003). Gaussian Particle Filtering. *IEEE Transactions on Signal Processing*, 51(10), 2592–2601.

Kraft, E. (2003). A Quaternion-Based Unscented Kalman Filter for Orientation Tracking. In *Proceedings of the Sixth International Conference of Information Fusion*, volume 1, 47–54.

Li, K., Frisch, D., Noack, B., and Hanebeck, U.D. (2019a). Geometry-Driven Deterministic Sampling for Nonlinear Bingham Filtering. In *Proceedings of the 2019 European Control Conference (ECC 2019)*. Naples, Italy.

Li, K., Frisch, D., Radtke, S., Noack, B., and Hanebeck, U.D. (2018a). Wavefront Orientation Estimation Based on Progressive Bingham Filtering. In *Proceedings of the IEEE ISIF Workshop on Sensor Data Fusion: Trends, Solutions, Applications (SDF 2018)*.

Li, K., Kurz, G., Bernreiter, L., and Hanebeck, U.D. (2018b). Nonlinear Progressive Filtering for SE(2) Estimation. In *Proceedings of the 21st International Conference on Information Fusion (Fusion 2018)*. Cambridge, United Kingdom.

Li, K., Pfaff, F., and Hanebeck, U.D. (2019b). Geometry-Driven Stochastic Modeling of SE(3) States Based on Dual Quaternion Representation. In *Proceedings of the 2019 IEEE International Conference on Multisensor Fusion and Integration for Intelligent Systems (MFI 2019)*. Taipei, Republic of China.

Li, K., Pfaff, F., and Hanebeck, U.D. (2019c). Hyperspherical Deterministic Sampling Based on Riemannian Geometry for Improved Nonlinear Bingham Filtering. In *Proceedings of the 22nd International Conference on Information Fusion (Fusion 2019)*. Ottawa, Canada.

Li, K., Pfaff, F., and Hanebeck, U.D. (2020). Grid-Based Quaternion Filter for SO(3) Estimation. In *Proceedings of the 2020 European Control Conference (ECC 2020)*. Saint Petersburg, Russia.

Mardia, K.V. and Jupp, P.E. (2009). *Directional Statistics*, volume 494. John Wiley & Sons.

Menegaz, H.M.T., Ishihara, J.Y., and Kussaba, H.T.M. (2019). Unscented Kalman Filters for Riemannian State-Space Systems. *IEEE Transactions on Automatic Control*, 64(4), 1487–1502.

Möls, H., Li, K., and Hanebeck, U.D. (2020). Highly Parallelizable Plane Extraction for Organized Point Clouds Using Spherical Convex Hulls. In *Proceedings of the 2020 IEEE International Conference on Robotics and Automation (ICRA 2020)*. Paris, France.

Pfaff, F., Li, K., and Hanebeck, U.D. (2020). The Spherical Grid Filter for Nonlinear Estimation on the Unit Sphere. In *Proceedings of the 21st IFAC World Congress (IFAC 2020)*. Berlin, Germany.

Smith, A. (2013). *Sequential Monte Carlo Methods in Practice*. Springer Science & Business Media.

Van Der Merwe, R., Doucet, A., De Freitas, N., and Wan, E.A. (2001). The Unscented Particle Filter. In *Advances in Neural Information Processing Systems*, 584–590.

Wan, E.A. and Van Der Merwe, R. (2000). The Unscented Kalman Filter for Nonlinear Estimation. In *Proceedings of the IEEE Adaptive Systems for Signal Processing, Communications, and Control Symposium*, 153–158.

Zhou, J., Yang, Y., Zhang, J., and Edwan, E. (2011). Applying Quaternion-Based Unscented Particle Filter on INS/GPS with Field Experiments. *Proceedings of the ION GNSS, Portland*, 1–14.